Journal Ovonic Research Vol. 3, No. 5, October 2007, p. 111 - 118

PHOTO DOPING EFFECTS OF SILVER ON ELECTRICAL PROPERTIES OF AMORPHOUS-ANTIMONY SELENIDE

Sanjeev Gautam[1], Navdeep Goyal
Centre of Advanced Study in Physics, Panjab University Chandigarh-160 014.

The effect of silver doping in a-Sb_2Se_3 in the temperature range 240-340 K and frequency range 0.5-100 kHz has been investigated for the variation of transport properties with optical doping. Silver doping is very distinct in case of optical doping as compared to thermal doping. E_g variation and voltage dependence are also studied for device applications of sample.

(Received October 5, 2007; accepted October 31, 2007)

Keywords: Amorphous semiconductors, dc conductivity, activation energy

1. Introduction

Chalcogenide glasses have a large number of applications and their use as photoresists for submicron technology is an added advantage [1–3]. These glasses can be easily thermal/photo doped with Ag and are useful as sensors [4] and voltage variable capacitors [5]. Formation of homogeneous phase during photo-dissolution of Ag is explained by Raman and others [4-14] to explore the structure of chalcogenide glasses. Various effects are studied on films [8, 9] as well as on bulk material [8, 10, 12–14]. Ag doping also shows applications in super-conducting [6] and magnetic materials [7].

The author therefore made some interesting study of conductance and capacitance under dark and illuminated conditions for Ag-Sb_2Se_3 at different temperature (230–340 K) and over a wide range of frequencies (5 Hz to 100 kHz). The measurements on Ag–Sb_2Se_3 indicate that Ag–based chalcogenide is sensitive to thermal and electrical stresses and hence could be used in device applications. The observed sensitivity is seemingly due to a wide distribution of gap states (including D^+-D^-) whose existence is supported through present measurements. The origin of D^+-D^- states could perhaps be due to heavy concentration of silver (as Ag^+ ions) in the material. Further, possible applications of Ag-Sb_2Se_3 as a diode junction and optoelectronic switch have also been studied.

2. Experimental details

The Chalcogenide glasses were prepared by melt quenching technique [16]. The pellets were prepared by compressing the finely grounded powder of a-Sb_2Se_3 to maximum compactness to form circular pellets having approximately same dimensions (diameter 0.677 cm, thickness 0.040 cm). The doping of silver into the host material was carried out optically on two dfferent pellets i.e. both the faces of pellet were coated with silver paste (≈10-20 μm) and then kept under special designed Ultra Violet (UV) source so that heat effct on pellet is negligible. Thereafter the optical treated pallet is kept in black paper tightly during all the measurements. Another pellet (virgin sample) was coated on both sides with aquadag (a commonly used conducting emulsion) for ohmic contacts [15]. The ohmic contacts were confirmed through linear I-V characteristics in

[1]Corresponding Author: sgautam@pu.ac.in (S. Gautam)

the voltage range for all pellets treated differently.

Measurements of impedance parameters of samples were made on an A.C. Impedance and C-V measurement System (Model 368 and 410, EG & G, PARC, USA) [16]. All electrical measurements of real and imaginary components of impedance parameters (Z′ and Z′′) and real and imaginary components of admittance parameters (Y′ and Y′′) were made over a wide range of temperature (230–340 K) and frequency (5 Hz–100 kHz).

3. Results and discussion

3.1 DC Conductivity of photo-doped Ag–Sb_2Se_3

The value of d.c. conductivity has been obtained from I-V characteristics at different temperatures. Figure 1 shows the plots of ln σ_{dc} versus 1000/T for undoped (a–Sb_2Se_3), thermally and photo doped (Ag–Sb_2Se_3) system. The graph obeys the pattern given by the expression [17]

$$\sigma_{dc} = C' \exp(-\Delta E/kT) \quad (1)$$

where ΔE and k are activation energy of the material and Boltzman's constant respectively. The plot for Ag–Sb_2Se_3 is found to be linear over the temperature range studied and has single activation energy 0.42±0.01 eV. In case of thermal doping the activation energy decreases to 0.26±0.01 eV [18], while for photo doping it decreases to 0.37±0.01 eV only.

3.2 Dipolar Behaviour of Photo-doped Ag–Sb_2Se_3

The Nyquist plots (Z′ versus Z′′) at different temperatures are drawn in Fig. 2. The semi-circular plots indicate the dipolar nature of the sample. Single semicircles are observed, as reported in case of undoped (a–Sb_2Se_3) sample, while two intersecting semicircles were

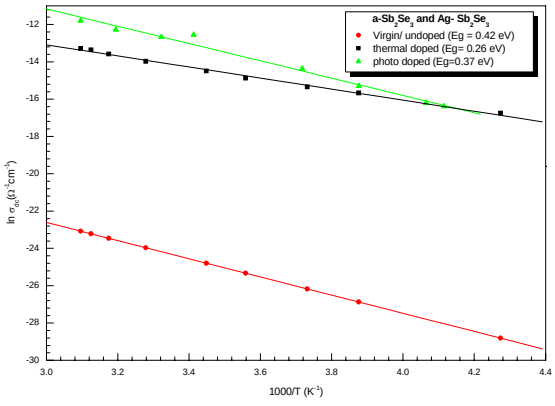

Fig. 1. Behaviour of DC conductivity for virgin with thermal and photo doped Ag-Sb_2Se_3..

observed in case of thermal doping (Ag–Sb_2Se_3) [18]. The photo doping increases the impedance of the material from 9.45×10^4 Ω to 20.5×10^4 Ω, while in case of thermal doping it is approximately same for doped part of the sample, as shown in the Fig. 3. In case of thermal doping, two clearly separable arcs are visible which is absent in case of photo-doped

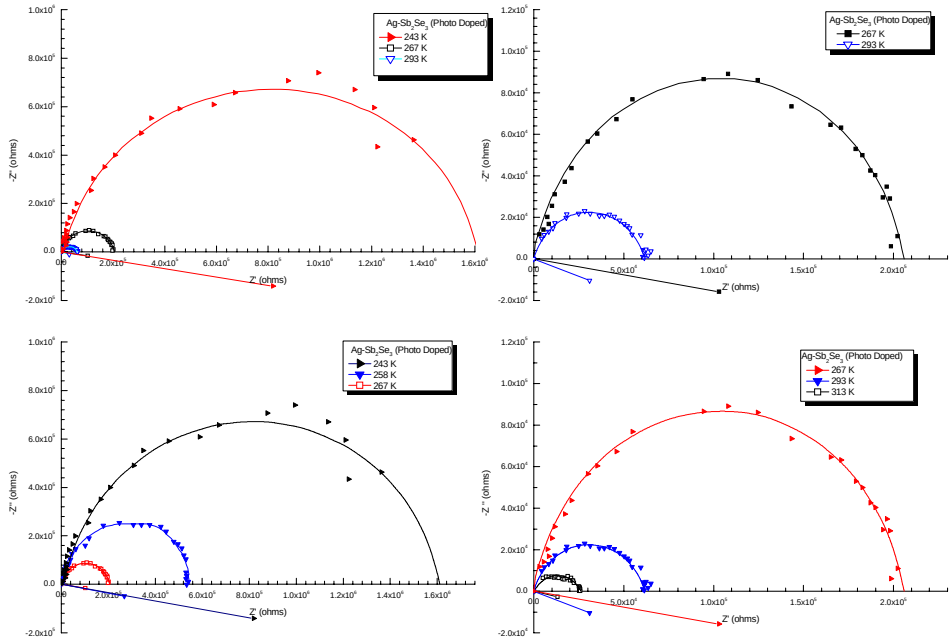

Fig. 2: Nyquist plots at different temperatures.

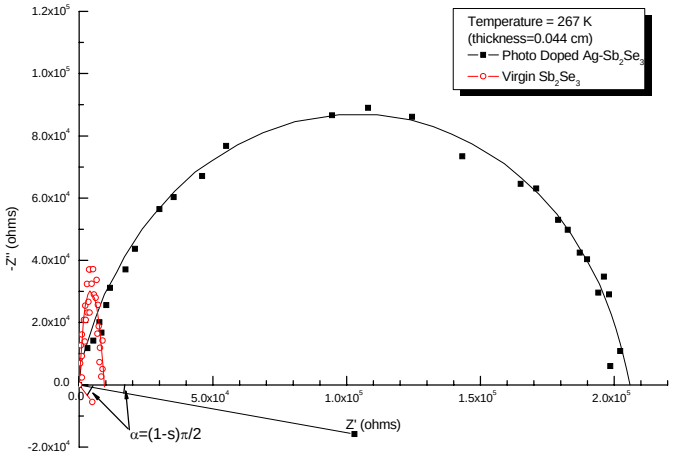

Fig. 3: Nyquist plots at 267 K for undoped (a–Sb_2Se_3) and doped Ag–Sb_2Se_3.

sample. Although photo doping increases the impedance of the sample like thermal doping. Figs. 4 and 5 show the Nyquist plots at different temperatures. The semicircular plots indicate the dipolar nature of the material. The area under the curve is decreasing with increase in temperature. The Nyquist plots drawn are semicircular arcs with their center lying below abscissa at an angle with their center lying below abscissa at an angle [$\alpha = (1 - s)\ \pi/2$] (i.e., the distribution). Such a behavior is typical of a dielectric system involving multi-relaxing process. However, for the photo doped system, Nyquist plot consist of single well defined arc, which is not starting from the origin. This can be explained with a series resistance in the R-C circuit as shown in Fig. 6. A series

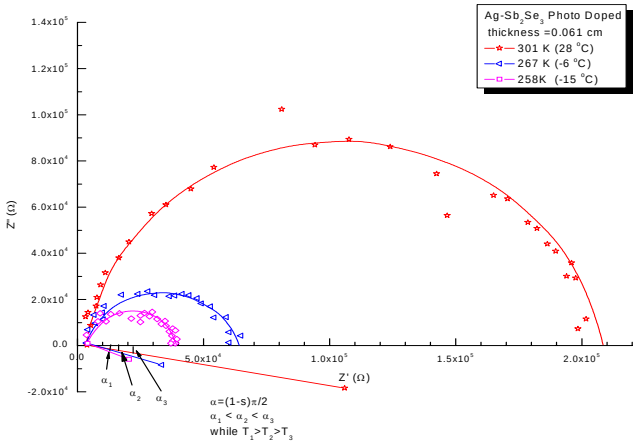

Fig. 4: Nyquist lots at 301, 267 and 258 K photo-doped Ag-Sb_2Se_3.

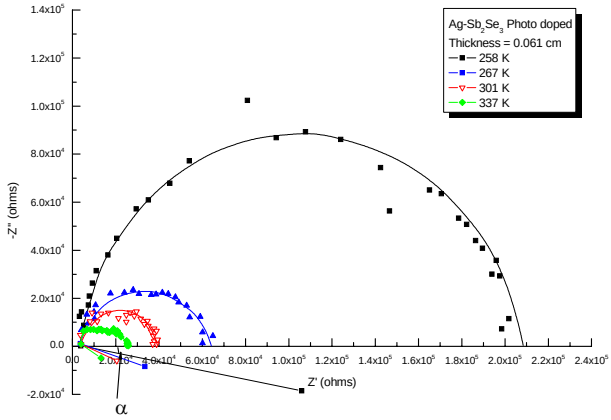

Fig. 5: Nyquist plots at 337, 301, 267 and 258 K photo-doped Ag-Sb_2Se_3.

resistance (R_s) is introduced after photo-doping to Ag-Sb_2Se_3, while in case of thermal doping one more parallel R-C circuit is formed. The arc describes the barrier due to $Ag^+[Sb_2Se_3]^-$. The real and imaginary components of impedance for such a system are given by

$$z' = R_s + \frac{R_p}{1 + \omega^2 R_p^2 C_p^2} \tag{2}$$

and

$$z'' = -\frac{\omega C_p R_p^2}{1 + \omega^2 R_p^2 C_p^2} \tag{3}$$

This type of behavior represents a clear separation of time constant $G_1/C_1 >> G_2/C_2$, with $G_1 << C_2$ and $G_2 << C_1$ [19].

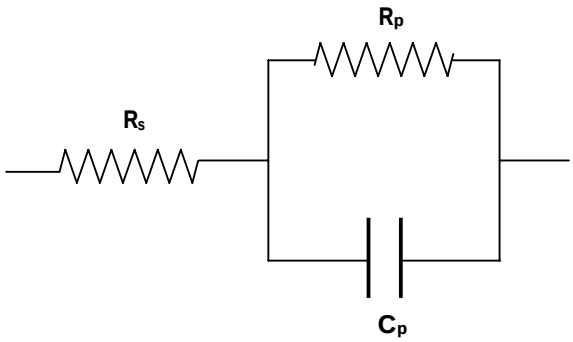

Fig. 6: R-C Circuit explaining the photo-doped Ag–Sb_2Se_3..

Likewise, the real and imaginary components of admittance are

$$Y' = G_p/\omega \quad and \quad Y'' = \omega C_p$$

Where G_p (=1/R_p) and C_p are the conductance and capacitance of the sample; ω is the angular frequency and R_s and R_p are series and parallel resistance respectively (Fig. 6), which is a characteristic feature of the sample system.

3.3 Voltage Effects in Photo-doped Ag–Sb_2Se_3

The voltage dependence on the Nyquist plots near room temperatures (293 and 298 K) is plotted in Figs. 7 and 8. The well defined semicircle is reduced on applying the voltage on the sample and regains its original size, as the voltage is removed. The data indicates the decrease in impedance with increase in the voltage, as discussed earlier. The similar effect has also been observed in case of thermal doping. The voltage effects on Nyquist plots is also investigated at lower temperature 293 K (Fig. 7) and found the similar effect on the sample.

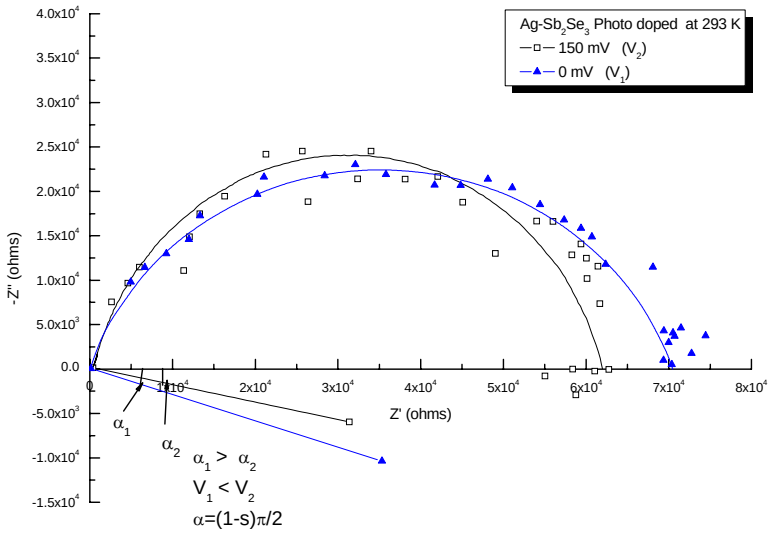

Fig. 7. Voltage dependence (0-150 mV) of photo-doped Ag-Sb_2Se_3.

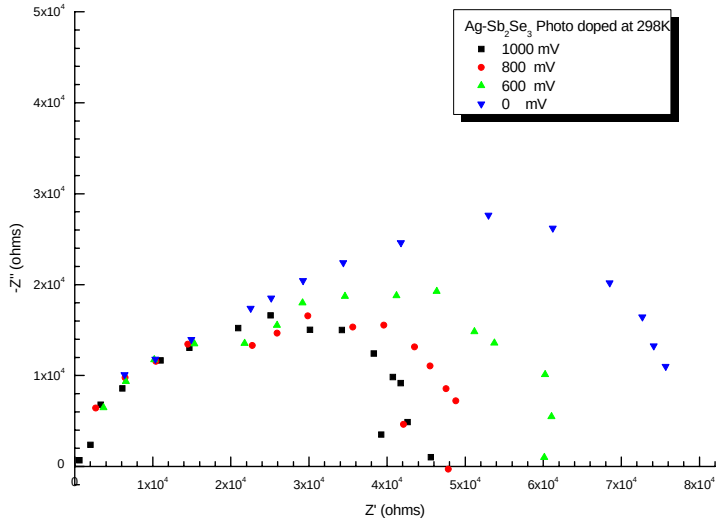

Fig. 8: Voltage dependence (0-1000 mV) of photo-doped Ag-Sb_2Se_3.

The variation of capacitance with log ω (Hz) at different temperatures is drawn in Fig. 9 and also capacitance variation with temperature is plotted in Fig. 10. The capacitance behavior is similar as obtained for the thermal doped sample.

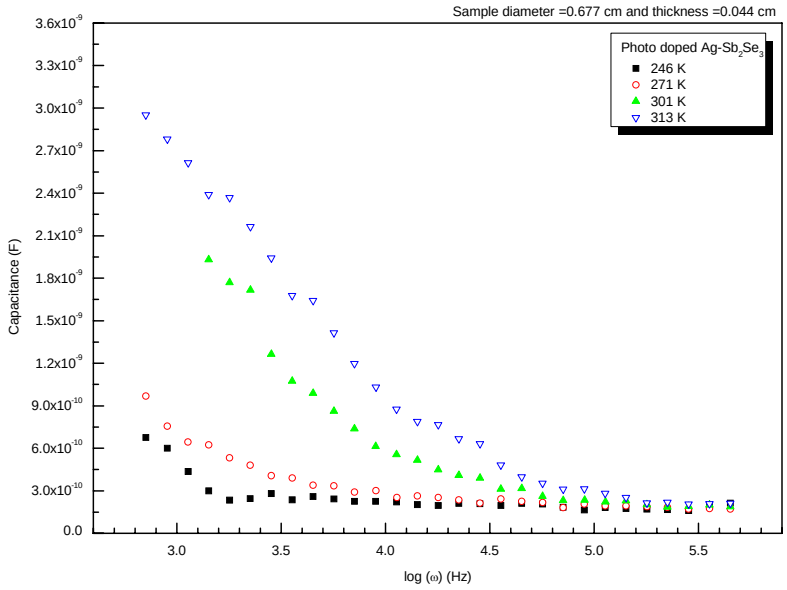

Fig. 9. Variation of capacitance with log ω (Hz) of photo-doped Ag-Sb_2Se_3 at different temperatures.

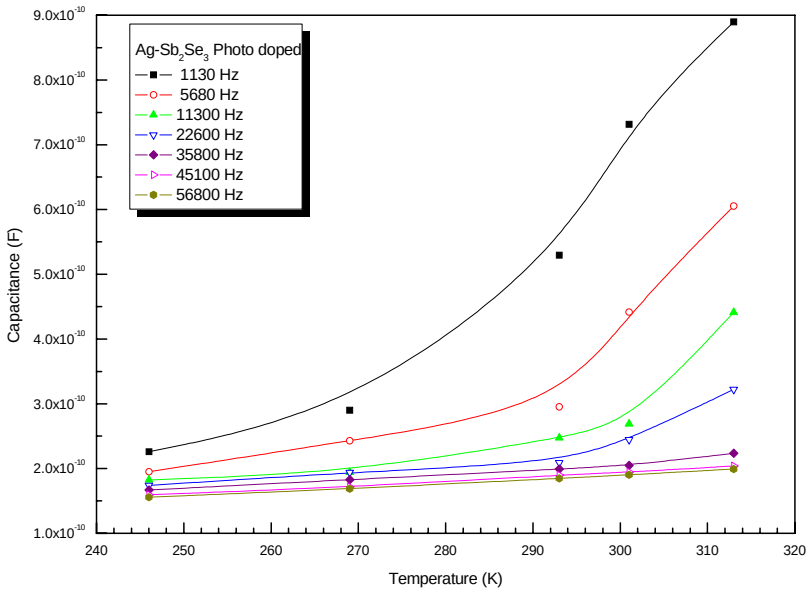

Fig. 10. Variation of capacitance with temperature of photo-doped Ag-Sb_2Se_3 at different frequencies.

3.4 Temperature and Frequency Dependence

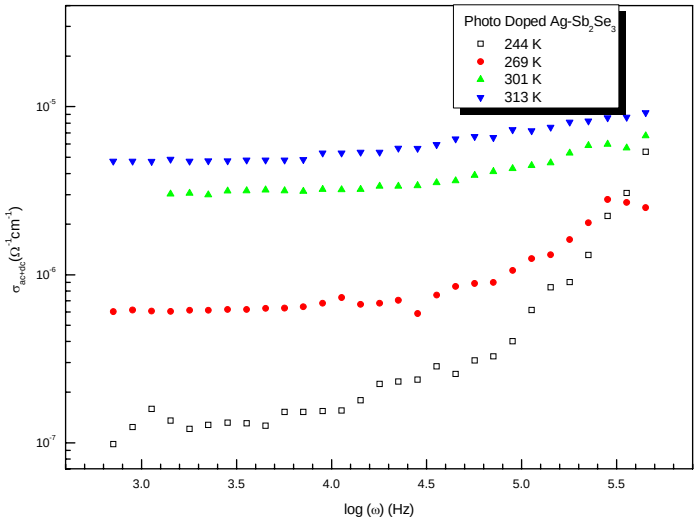

Fig. 11. Variation of ln σ_{ac+dc} (Ω^{-1} cm^{-1}) with log ω (Hz) for photo-doped Ag-Sb_2Se_3.

Fig. 11 shows the frequency dependence of total conductivity [σ(ω)] at different temperatures for photo-doped Ag-Sb_2Se_3. It is evident from the figure that with decreasing temperatures σ(ω) becomes more and more frequency dependent. This is understandable because at lower temperatures the a.c. conductivity starts dominating over the d.c. component.

4. Conclusions

Nyquist plots or complex impedance studies confirm the dipolar nature of a-Sb_2Se_3 and multi-relaxation behavior as seen in most of chalcogenide glasses. These plots also indicate that the capacitive nature dominates over the resistive nature of the sample at lower temperature (<273 K), while the resistive nature is dominant at higher temperatures. The conduction mechanism has a shift from bipolaron to single polaron hopping (276-278 K). The temperature and frequency dependence of a.c. conductivity is well explained by the m-CBH model. The contribution to a.c. conductivity from single polaron hopping is dominant at higher temperatures. In both the doping techniques the formation of two homogenous phases occurs, one is doped and other is undoped. In case of thermal doping the doped and undoped parts are separable or more refine. The dopant has not gone to more depth into the sample, while in case of optical doping the doped and undoped part are of equal resistance and are non-distinguishable at room temperature. Thermal doping in the system Ag–Sb_2Se_3 produces two distinct phases, which are clearly visible at lower temperatures. The optical doping also changes the impedance of the sample. In this case Ag^+ goes deep inside the bulk, but doping concentration seems to be less.

Acknowledgements

SG is thankful to Panjab University Experimental High Energy Physics (PU-EHEP) Group, for their support.

References

[1] K. L. Tai, E. Ong, R. G. Vadmisky, Proc. of Electrochem. Society **82**, 9 (1982).
[2] A. P. Firth, P. J. S. Ewen, C. M. Huntley, Adv. in Resis Tech. and Processing II, Proc. SPIE **539**, 160 (1985).
[3] H. S. Rennie, S. R. Elliott, J. Non-Cryst. Solids **77**, 1161 (1985).
[4] K. K. Srivastva, A. Vohra, Phil. Mag. **64**, 201 (1990).
[5] P. Khurana, K. K. Srivastva, Indian J. Pure Appl. Phys. **28**, 393 (1990).
[6] N. Kamakura, T. Nakano, Y. Ikemoto, M. Usuda, H. Fukuoka, S. Yamanaka, S. Shin, K. Kobayashi, Phys. Rev. B **72**, 014511 (2005).
[7] Q. Y. Xu, R. P. Wang, Z. Zhang, Phys. Rev. B **71**, 092401 (2005).
[8] M. Frumar, T. W´agner, Current Opinion in Solid State and Mat. Sc. **7**, 117 (2003).
[9] H. Jain, A. Kovalskiy, A. Miller, J. Non-Cryst. Solids **352**, 562 (2006).
[10] Y. Takano, K. Hirata, M. Senda, M. Kitao, S. Yamada, J. Non-Cryst. Solids **77/78**, 1245 (1985).
[11] P. L. Sherrell, J. C. Thompson, J. Non-Cryst. Solids **24**, 69 (1977).
[12] A. Tamai, A. P. Seitsonen, R. Fasel, Z. -X. Shen, J. Osterwalder, T. Greber,Phys. Rev. B **72**, 085421 (2005).
[13] P. W. Anderson, Phys. Rev. **109**, 1492 (1958).
[14] N. F. Mott, Adv. Phys. **16**, 49 (1967).
[15] S. Gautam, D. K. Shukla, S. Jain, N. Goyal, Parmana J. Phys. **50**(1), 25 (1998).
[16] Navdeep Goyal, Parmana J. Phys. **40**, 97 (1993).
[17] N. F. Mott, A. Davis, Electronic processes in Non-Crystalline Materials, Clarendon Press, Oxford, England, (1971).
[18] S. Gautam, Anup Thakur, S.K. Tripathi and Navdeep Goyal, J. Non-Cryst. Solids **353**, 1315–1321 (2007).
[19] A. K. Jonscher, Dielectric Relaxation in Solids, Chelsa Dielectric Press, London, (1983).